

Supplemental Materials

Molecular Biology of the Cell

Fu et al.

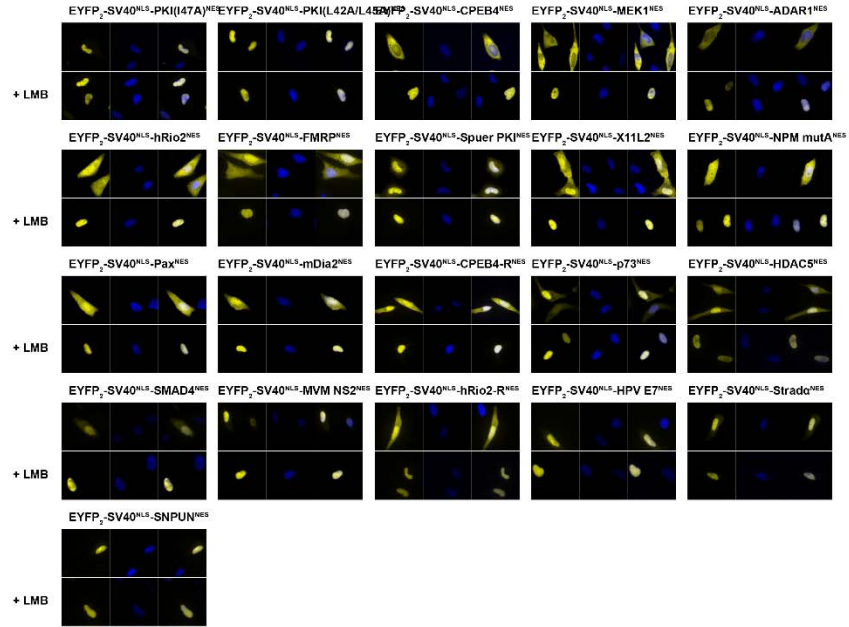
CRM1-MVM NS2^{NES} structure determination

Full-length wild type ^{Hs}CRM1, ^{Sc}CRM1 mutant for crystallization (residues 1-1058, Δ377-413, T539C, V441D), human Ran and ^{Sc}RanBP1 (Yrb1p) was expressed and purified as previously described in as previous chapters. Complex formation, crystallization and structural determination were performed as described in previous study (Fung *et al.*, 2015). X-ray diffraction data was collected at Advanced Photon Source (APS) – Structural Biology Center (SBC) 19ID beamline. Data was processed and refined using the same procedure as described in earlier chapters. MVM NS2^{NES} peptide was modeled according to the positive difference density (2mFo-DFc map) at the binding groove after refinement of the CRM1-Ran-RanBP1 model. The good side-chain densities for Φ residues allowed unambiguous sequence assignment. The refined model also fits kick OMIT density perfectly as shown in Figure 3B. Kick OMIT density was calculated in PHENIX by omitting the NES peptide.

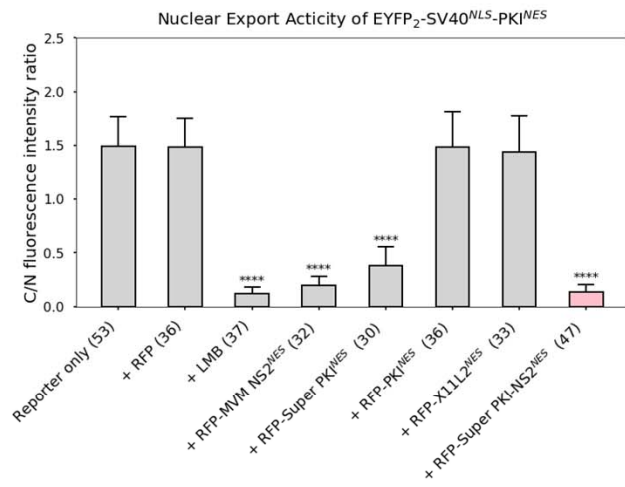
Data simulation in PALMIST

In order to estimate the limit of detection of K_D s in our experimental set-up, data was simulated using parameters from the titrations in Figure 3D and varying affinities of MBP-NES, and loaded back into PALMIST for analysis. Data was simulated with noise of 1.0 unit with Gaussian distribution in triplicates. Simulated data using $K_D = 0.2$ nM failed to fit while data simulated with $K_D = 0.3$ nM and 0.5 nM yielded $K_D = 1$ [U, 4] nM and 1 [U, 6] nM respectively, both with undefined lower limits (Figure S3C). A K_D with both defined lower and upper limits can only be obtained when fitting data simulated using $K_D > 1$ nM. Curve shapes of the fitted isotherms for sub-nanomolar affinities have characteristic sharper turns as the relative fluorescence reaches the maximum when compared to the fitted isotherms with $K_D = 1-10$ nM. The data obtained and the fitted isotherms of experimentally collected data for MBP-Super PKI-NS2^{NES} and MBP-CDC7-NS2^{NES} both show sharp turns similar to data simulated for $K_D = 0.3$ nM (Figure 3D and Figure S3C). Our analysis of simulated data therefore supports the fitting of the experimental data that both NS2 fusion/chimeric mutants have a sub-nanomolar binding affinity.

A



B



C

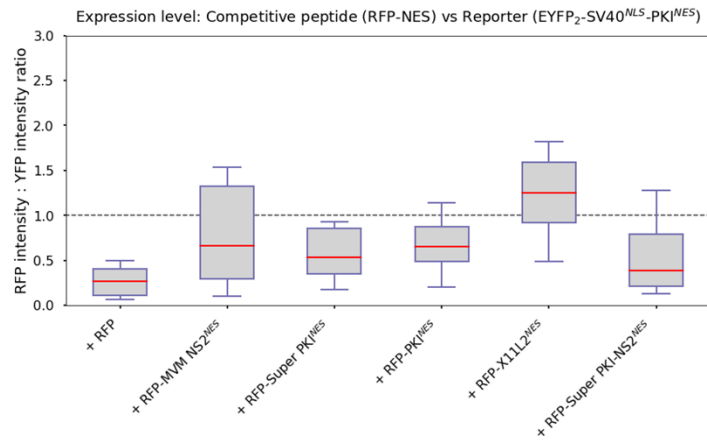
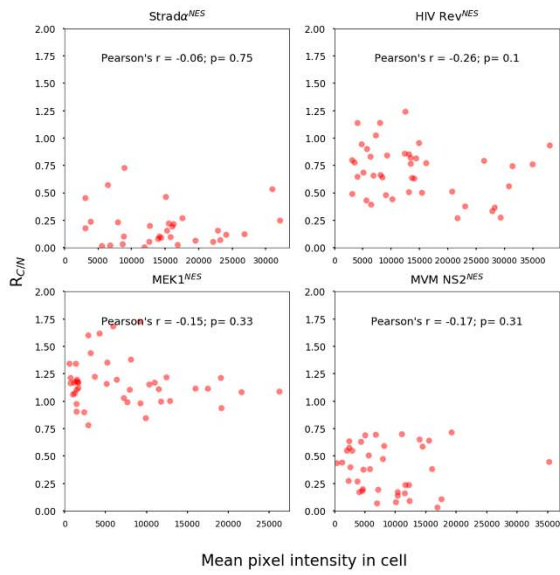
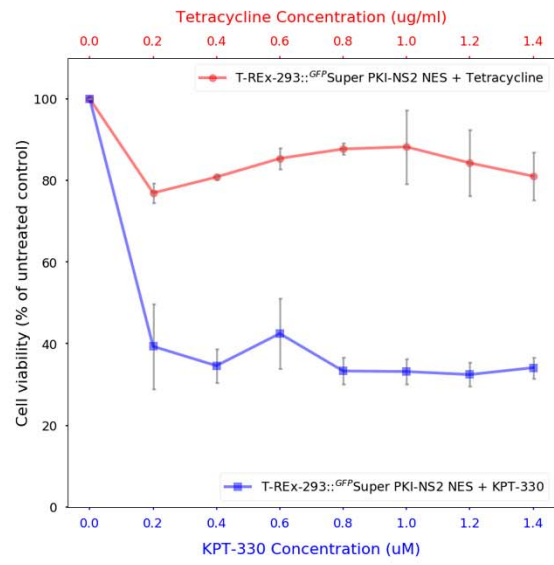


Figure S1. Leptomycin B (LMB) sensitive nuclear export activity of EYFP₂-SV40^{NLS}-NES in HeLa cells. (A) YFP (pseudocolored in yellow), Hoechst (pseudocolored in blue) images were captured using spinning disk confocal microscope (40x). CRM1-dependence is demonstrated by the nuclear accumulation after treatment with 5 nM leptomycin B (+LMB) for 16-18 h. **(B)** EYFP₂-SV40^{NLS}-PKI^{NES} is co-transfected with RFP, RFP-MVM NS2^{NES}, RFP-Super PKI^{NES}, RFP-PKI^{NES}, RFP-X11L2^{NES} or RFP-Super PKI-NS2^{NES} (pink bar) and compared with cells expressing EYFP₂-SV40^{NLS}-PKI^{NES} that are treated with small molecule inhibitor LMB. The numbers of examined cells from at least 3 independent experiments are indicated in parentheses. Error bars represent standard deviation, and P-values were calculated in comparison to control (reporter only) using Mann-Whitney tests. Note that observed R_{C/N} values are presented without normalization to compare with R_{C/N} upon LMB treatment (+LMB). **(C)** The expression ratio of RFP-tagged competitive peptide to EYFP₂-SV40^{NLS}-PKI^{NES} (reporter) in HeLa cells. The mean RFP and YFP intensities of the whole cell were measured in at least 10 independent cells from different experiments. Representative images of cells co-transfected with reporter proteins and competitive peptides were captured using spinning disk confocal microscope (40x) and shown in Figure 2C.

A



B



C

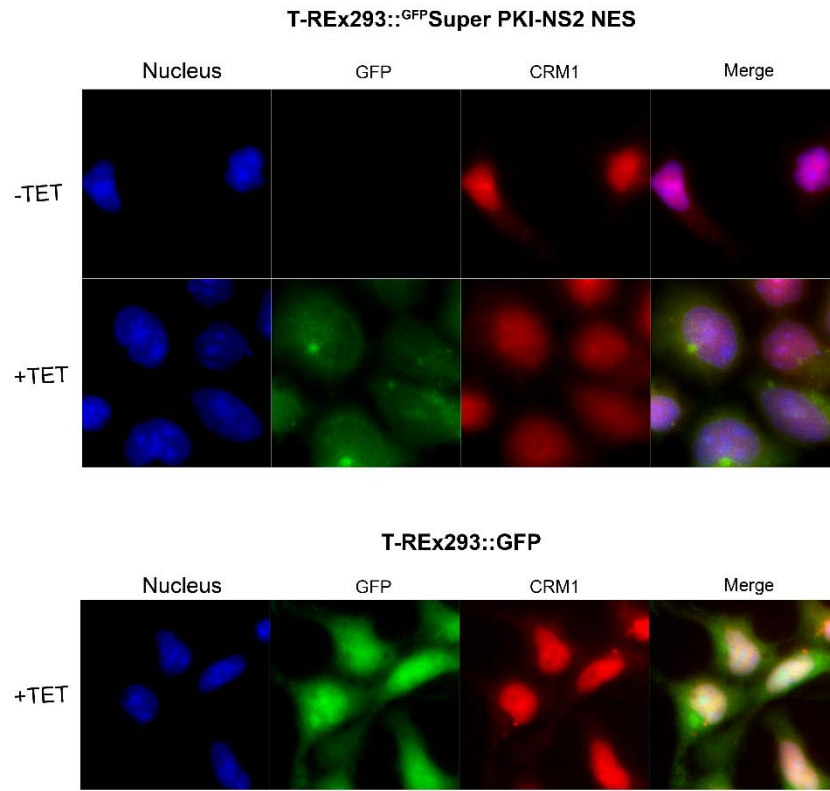


Figure S2. (A) The ratio of cytoplasmic to nuclear localization ($R_{C/N}$) is independent of EYFP₂-SV40^{NLS}-NES reporter expression in HeLa cells. To examine the impact of variation in expression level of reporter proteins among different cells, $R_{C/N}$ values are plotted for individual HeLa cells as a function of the mean fluorescence intensity of the whole cell. Results are shown for four different NESs that have different affinities for CRM1. (I) Stradd^{NES} ($K_D = 10300$ [8000, 13000] nM). (II) HIV Rev^{NES} ($K_D = 1180$ [990, 1400] nM). (III) MEK1^{NES} ($K_D = 70$ [40, 130] nM). (IV) MVM NS2^{NES} ($K_D = 2$ [U, 9] nM). U, limit of detection cannot be defined. **(B)** Cytotoxicity of Super PKI-NS2^{NES}. The graph represents the cytotoxicity profile of Super PKI-NS2^{NES} in a stable cell line that expresses Super PKI-NS2^{NES} in T-REx-293 cells using a tetracycline-inducible system (TET-on). Cell viability was determined by CCK-8 assay (Dojindo Inc., Japan). T-REx-293::^{GFP}Super PKI-NS2 NES cells were induced at different concentrations (0.2 -1.4 μ g/mL) on 48 h incubation. CRM1 inhibitor, Selinexor or KPT-330 (Karyopharm), was treated at different concentrations (0.2 -1.4 μ M) as positive control. Results are expressed as a percentage of untreated control \pm SEM from three independent experiments. **(C)** Super PKI-NS2^{NES} does not alter the subcellular localization of endogenous CRM1. Representative images of CRM1 immunostaining are shown. *Top panel*, CRM1 subcellular localization in the absence (-TET) and presence (+TET) of peptide inhibitor in T-REx-293::^{GFP}Super PKI-NS2 NES cells. *Bottom panel*, CRM1 subcellular localization in a control cell line: T-Rex-293::GFP. Endogenous CRM1 was detected by CRM1 antibody (C-1, Santa Cruz Biotechnology) at 1:50 dilution and imaged using a Deltavision pDV microscope (60x). Nuclear counter stain is pseudocolored in blue, GFP is in green and CRM1 is in red. For each channel, 21 nuclear z-planes spanning the middle of the nucleus (total z size 2 μ m) were selected and merged into a single image as described in Materials and Methods.

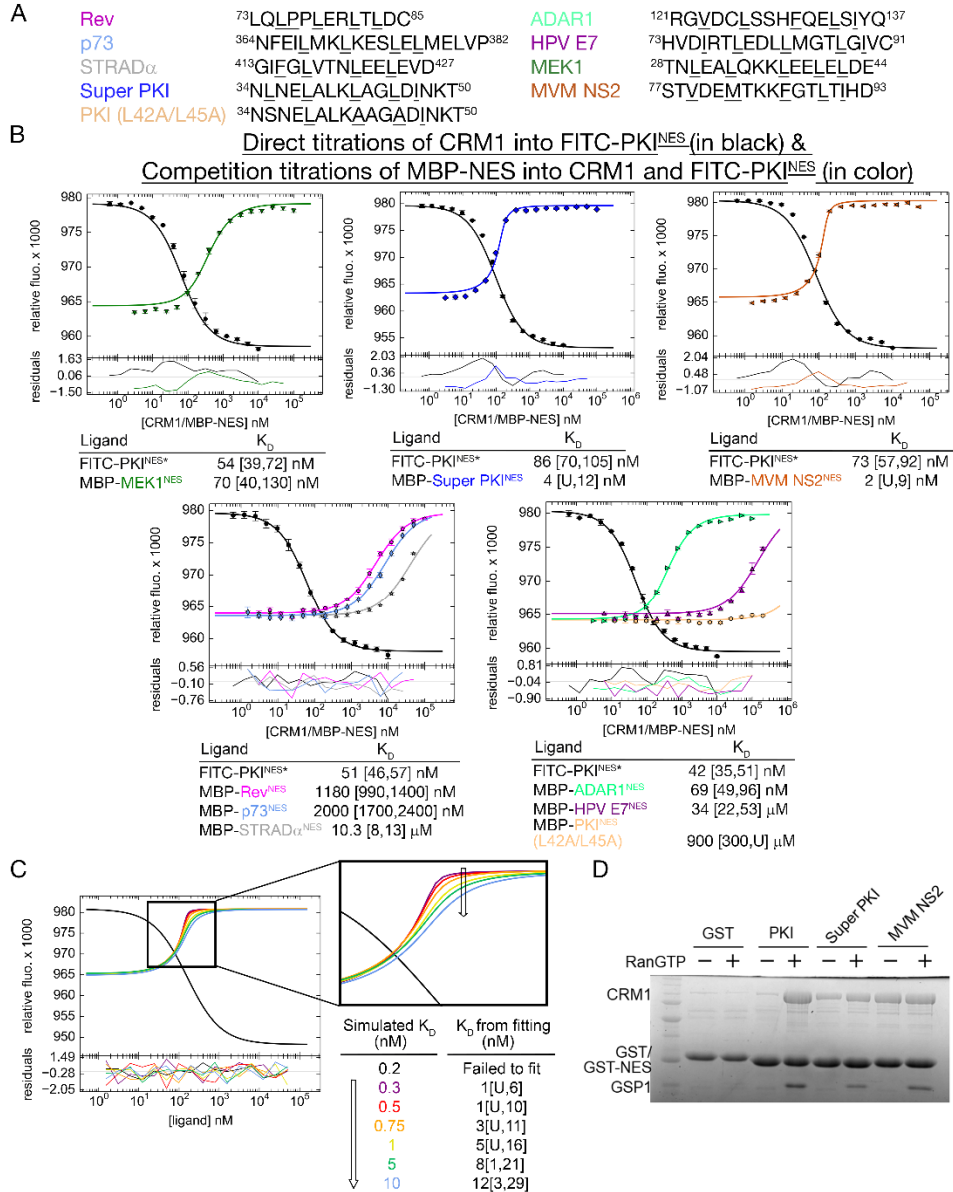


Figure S3. CRM1-NES Binding affinities measured by differential bleaching and additional CRM1 binding to high affinity NESs in the presence and absence of RanGTP. (A) Sequences of NES peptides used (Φ residues are underlined). **(B)** Data from triplicate experiments of direct titration of CRM1 to FITC-PKI^{NES} in presence of excess RanGTP (black) or competition titrations of MBP-NES to FITC-PKI^{NES} and CRM1 with excess RanGTP (color) are plotted as mean \pm SD. Fitted binding curves are overlaid and residuals are plotted. Dissociation constants (K_D) are reported with the 95% confidence interval in brackets. Experiments performed on different days were fitted using

the corresponding triplicate set of direct titrations. **(C)** Data simulation in PALMIST showing that the lower limit of detection of K_D is ~ 1 nM. Data is simulated in PALMIST using the K_D s indicated on the left and fitted to yield K_D s listed side-by-side on the right. Data points were not plotted for simplicity. Isotherms are colored in rainbow to indicate the shape change as the K_D increases. **(D)** High affinity NESs can bind CRM1 in the absence of RanGTP. Pull-down assays with ~ 1.3 μ M immobilized GST or GST-NESs and 2.5 μ M CRM1 with or without 7.5 μ M RanGTP. Reaction mixture was incubated for 30 mins, washed intensively and visualized with Coomassie-stained SDS-PAGE.

Table S1. Data collection and refinement statistics.

Data collection	
Crystal of CRM1-Ran-RanBP1 bound to:	MVM-NS2 ^{NES}
Space group	P4 ₃ 2 ₁ 2
Cell dimensions a=b, c (Å)	106.57, 304.08
Resolution range (Å)	50.00 – 2.03 (2.07 – 2.03)
Unique reflections	114290 (5641)
Multiplicity	10.1 (9.0)
Data completeness (%)	100 (100)
$R_{\text{merge}}/R_{\text{pim}}$ (%)	7.1 (132.7) / 2.3 (46.0)
$I/\sigma(I)$	31.4 (1.7)
$CC_{1/2}$ (last resolution shell)	0.591
Refinement statistics	
Resolution range (Å)	40.23 – 2.03 (2.08 – 2.03)
No. of reflections $R_{\text{work}}/R_{\text{free}}$	109505/2000 (4337/80)
Data completeness (%)	95.8 (79.0)
Atoms non-H protein/ligand and ions/H ₂ O	11083/70/867
$R_{\text{work}}/R_{\text{free}}$ (%)	18.8/21.5 (26.8/28.6)
R.m.s.d. Bond length (Å)/angle (°)	0.002/0.504
Mean B-value (Å ²) Protein Ligands and ions/H ₂ O NES peptide/ ϕ^a	35.8 34.5 57.5/48.6
Ramachandran plot (%) ^b favored /disallowed	97.83/0.00
ML coordinate error	0.21
Missing residues Chain A: Ran Chain B: RanBP1 Chain C: CRM1 Chain D: NES peptide	A: 1-8, 188, 189; B: 62, 70-77; C: 439-460, 1054-1058

PDB ID: 6CIT

Data for the outermost shell are given in parentheses.

^a B-factors for the entire NES peptide, B-factors for only Φ residues of the NES peptides (as indicated in the figures) and B-factors for the 29 CRM1 residues that line the NES-binding groove are also reported.

^b As defined by MolProbity in PHENIX.